APPENDIX A

Lithological Log

The well lithological log information that used in this study is located at 520840E 2070140N which is about 6.5 km in south-west direction away from the study area released by Department of Mineral Resources in 2003. The lithological log detail is presented in Table A.1.

Table A.1 shows the lithological log modified from Department of Mineral Resources report in 2003.

TG0180 (Log No.43463), UTM: 520840E 2070140N		
Ban Pa Ngae, On Tai Subdistrict, San Kamphaeng District, Chiang Mai		
Top	Bottom	Material types
0	4.5	Sand
4.5	10.5	Clay, Sand
10.5	19.5	Gravel
19.5	22.5	Clay
22.5	25.5	Gravel
25.5	28.5	Clay, Gravel
28.5	36.0	Gravel
36.0	49.5	Clay
49.5	52.5	Shale
52.5	60.0	Basalt
60.0	81.0	Basalt, Limestone

APPENDIX B

Reflection Seismic

The processing example results of Line MO-1 display in Figure B.1, Figure B.2, Figure B.3, Figure B.4, and Figure B.5. The processing example results of Line MO-3 display in Figure B.6, Figure B.7, Figure B.8, Figure B.9, and Figure B.10. The processing example results of Line MO-4 display in Figure B.11, Figure B.12, Figure B.13, Figure B.14, Figure B.15, and Figure B.16.
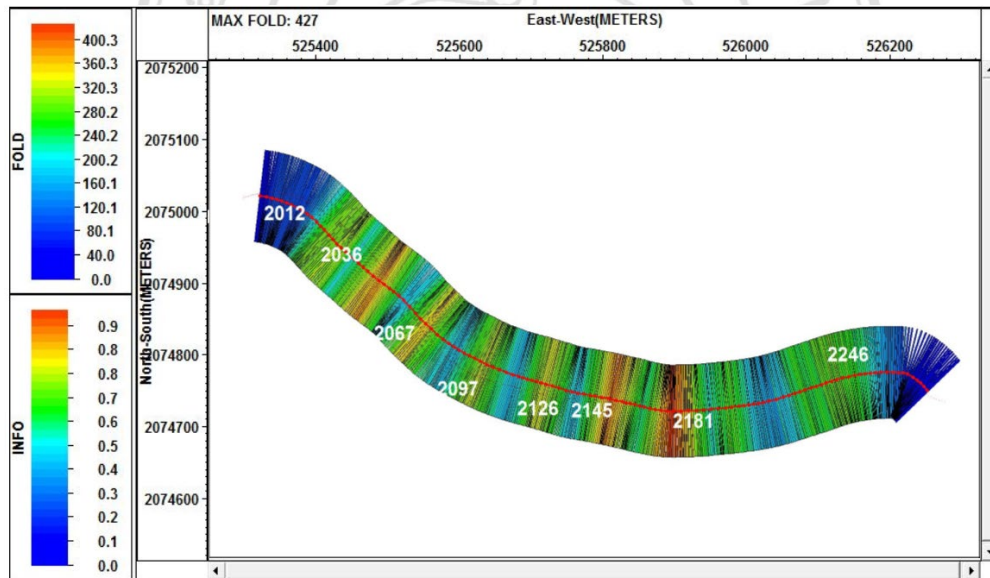

Figure B.1   displays the geometry setting of Line MO-1. The surface line shows in red circle. The bins show in rectangular area with 2×20 m^2 and color bar represents the fold coverage.
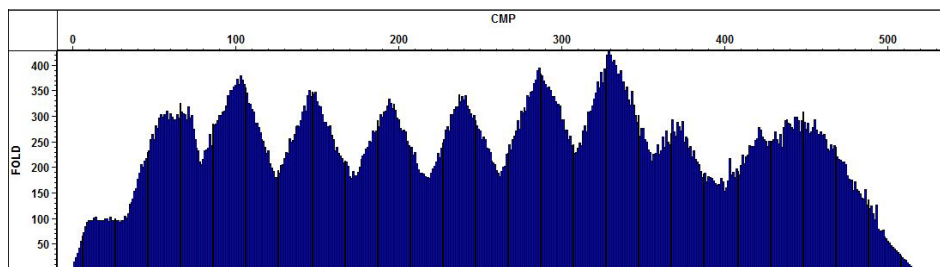

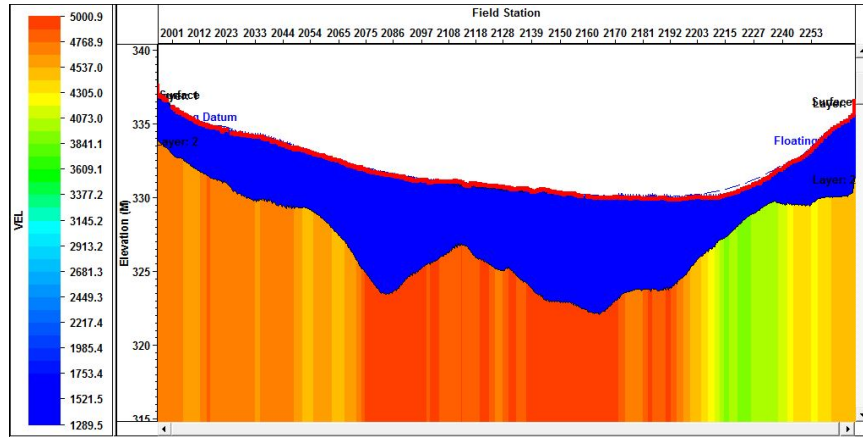Figure B.2   exhibits the total fold coverage of each CMP from Line MO-1.

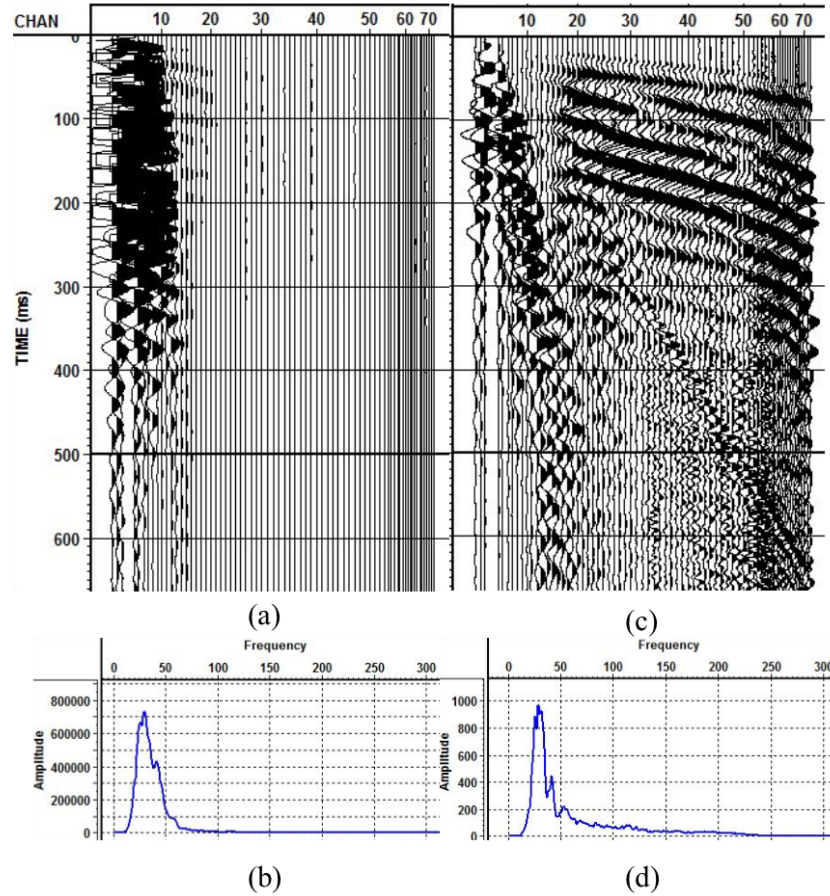Figure B.3   displays velocity model determined from first arrival time.

Figure B.4   shows example shot gather number 2590 from Line MO-1, (a) raw shot record with its average amplitude spectrum (b) and (c) shot gather after geometry setting, static correction, amplitude scaling and recovery with exponential constant 1 to compensate for attenuation loss and bandpass filter 10-20-200-250 Hz with its average amplitude spectrum in (d).
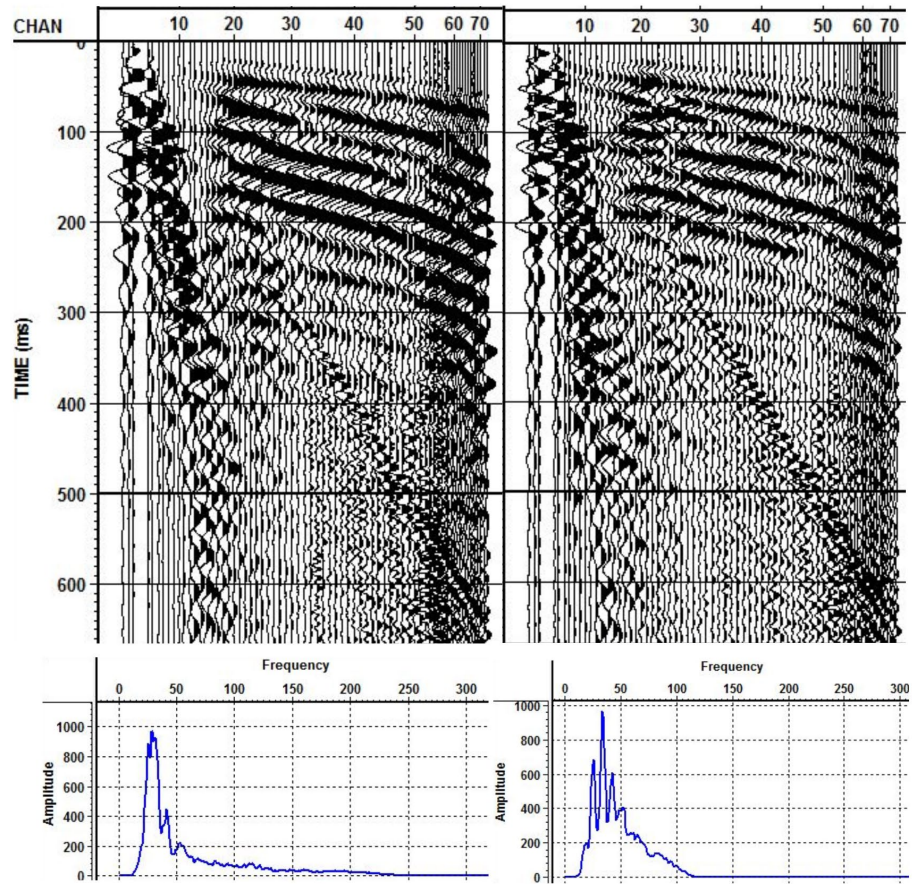
Shot 2590

Figure B.5   displays the shot gather number 2590 from Line MO-1 (left) after frequency filter 10-20-200-250 and (right) after surface consistent deconvolution with operator length 80 ms and predictive lag 12 ms follow by 10-20-90-120 bandpass filter and mean scaling.
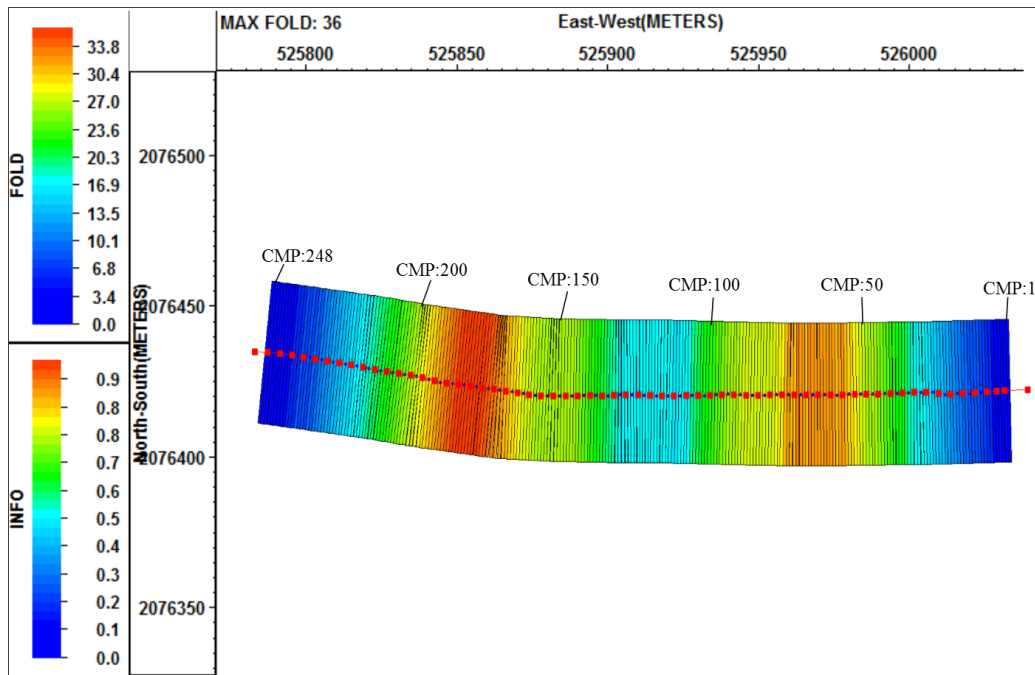
Figure B.6 displays the geometry setting of Line MO-3. The surface line shows in red circle. The bins show in rectangular area with 1×20 m^2 and color bar represents the fold coverage.
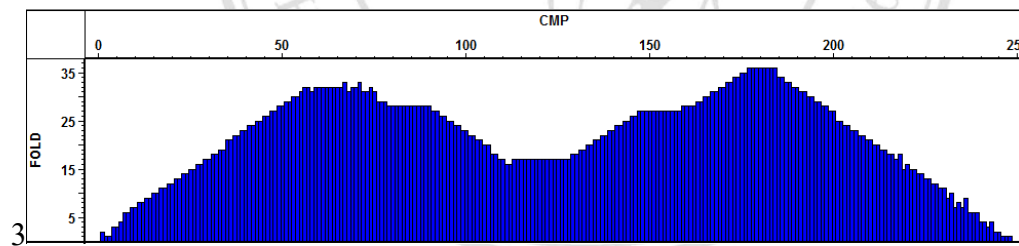

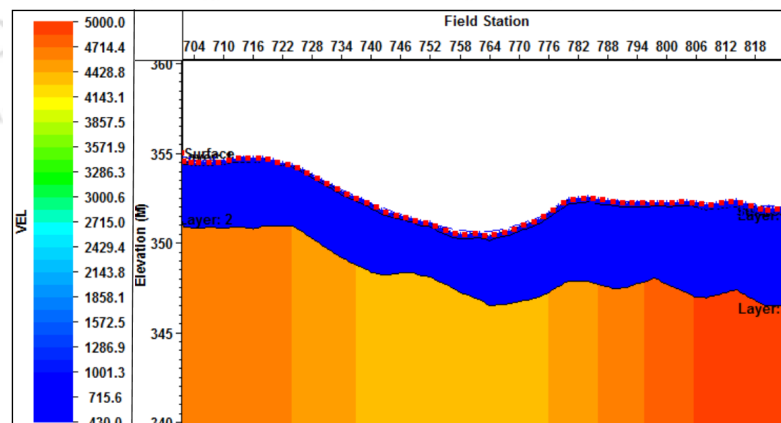Figure B.7 exhibits the total fold coverage of each CMP from Line MO-3

Figure B.8 displays velocity model determined from first arrival time of Line MO-3.
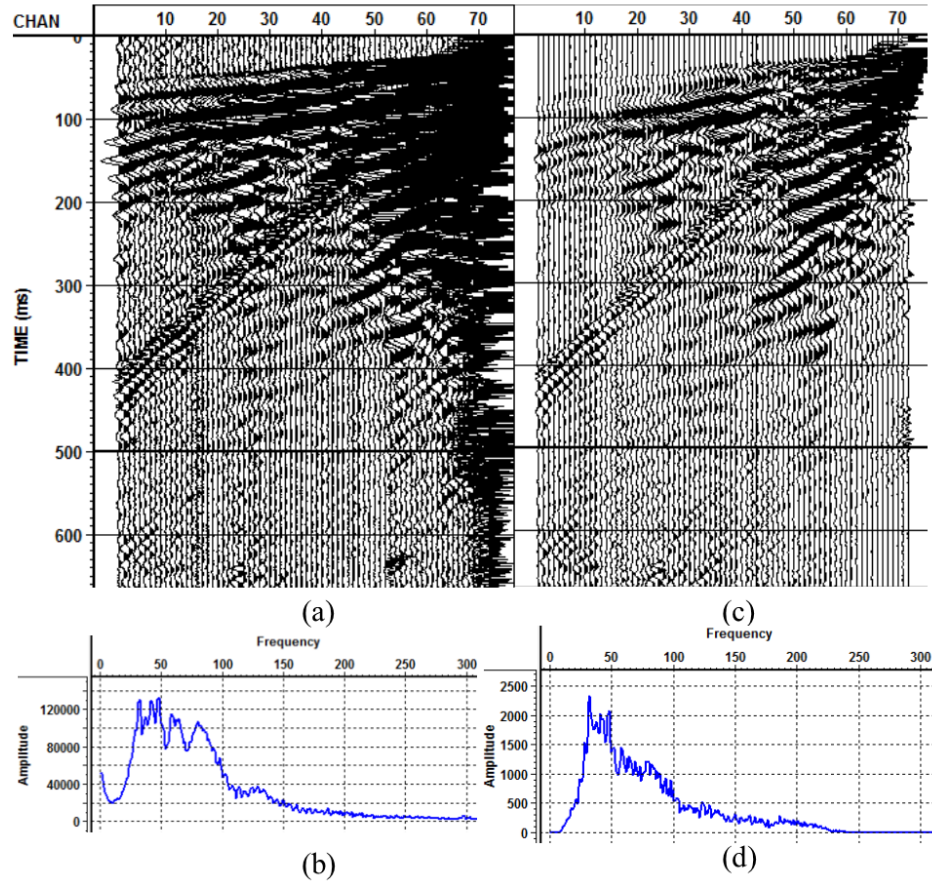
Shot 823

(a)   (b)   (c)   (d)

Figure B.9   shows example shot gather number 823 from Line MO-3, (a) raw shot record with its average amplitude spectrum (b) and (c) shot gather after geometry setting, static correction, amplitude scaling and recovery with exponential constant 1 to compensate for attenuation loss and bandpass filter 10-20-200-250 Hz with its average amplitude spectrum in (d).
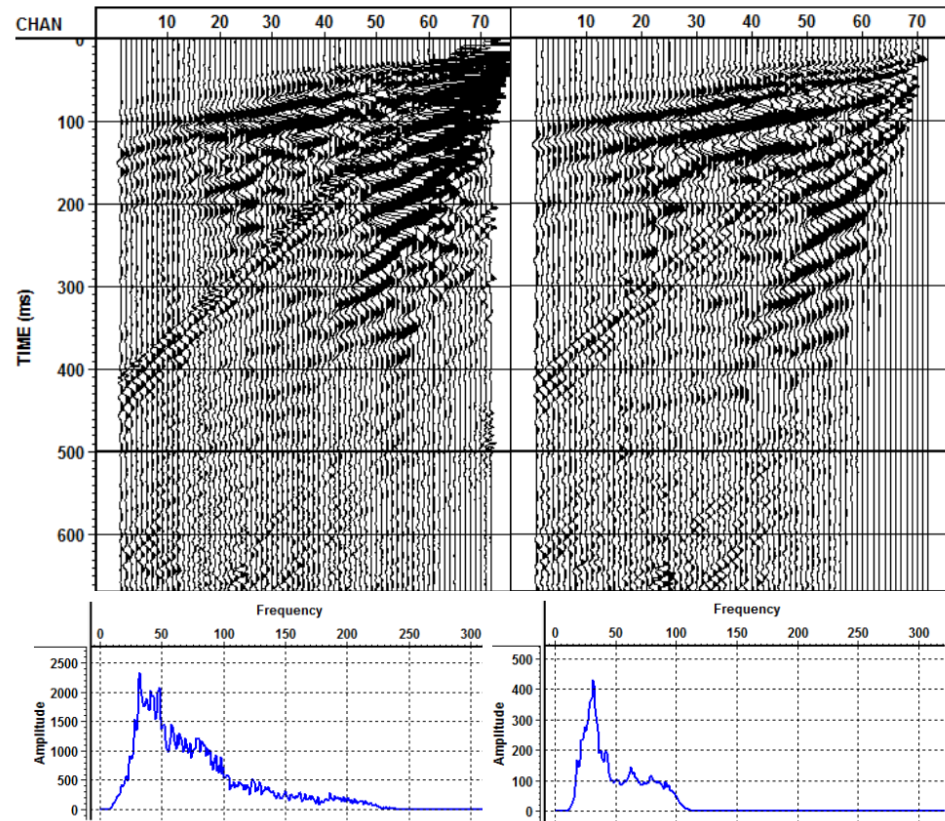
Shot 823

Figure B.10 displays the shot gather number 823 from Line MO-3 (left) after frequency filter 10-20-200-250 and then(right) after surface consistent deconvolution with operator length 80 ms and predictive lag 12 ms follow by by 10-20-90-120 bandpass filter, mean scaling and bottom mute.
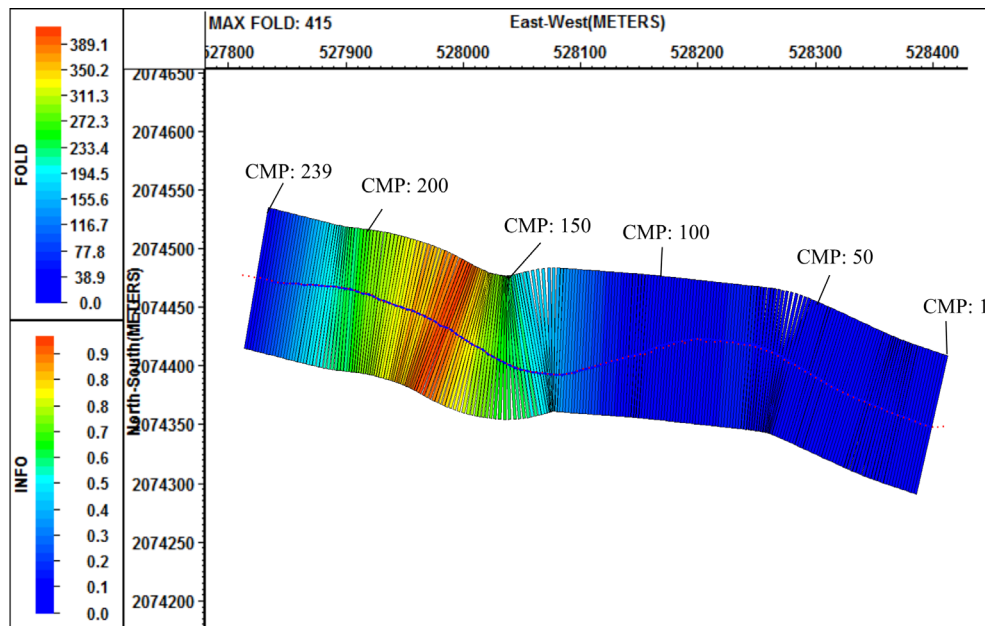
Figure B.11 displays the geometry setting of Line MO-4. The surface line shows in red circle. The bins show in rectangular area with 2.43×20 m^2 and color bar represents the fold coverage.
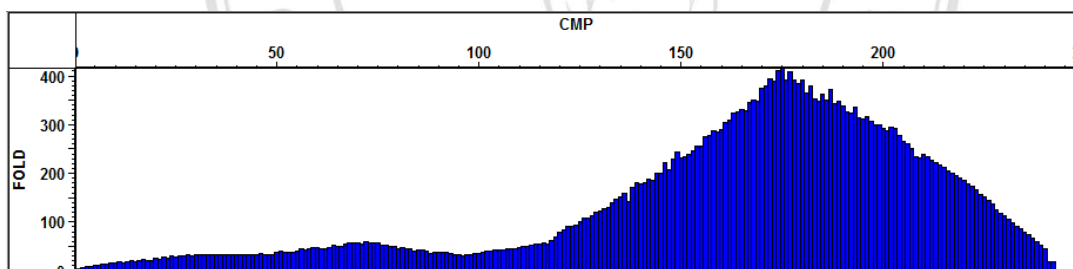

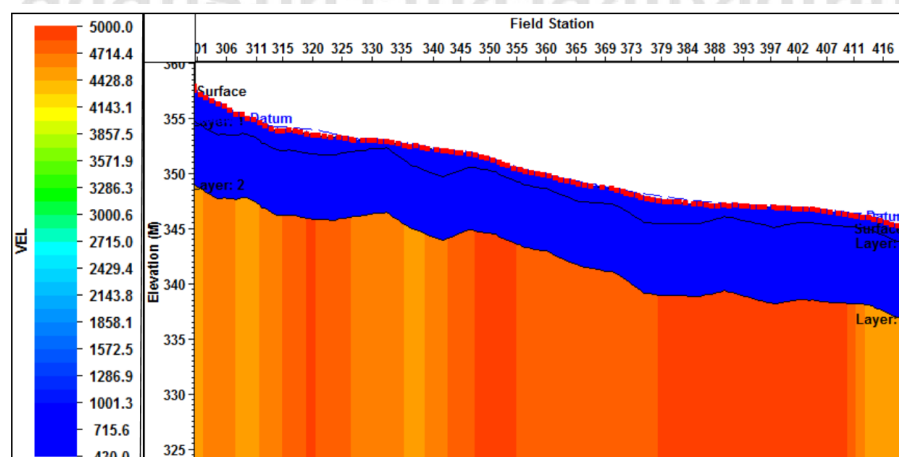Figure B.12 exhibits the total fold coverage of each CMP from Line MO-4

Figure B.13 displays velocity model determined from first arrival time of Line MO-4.

Shot 317
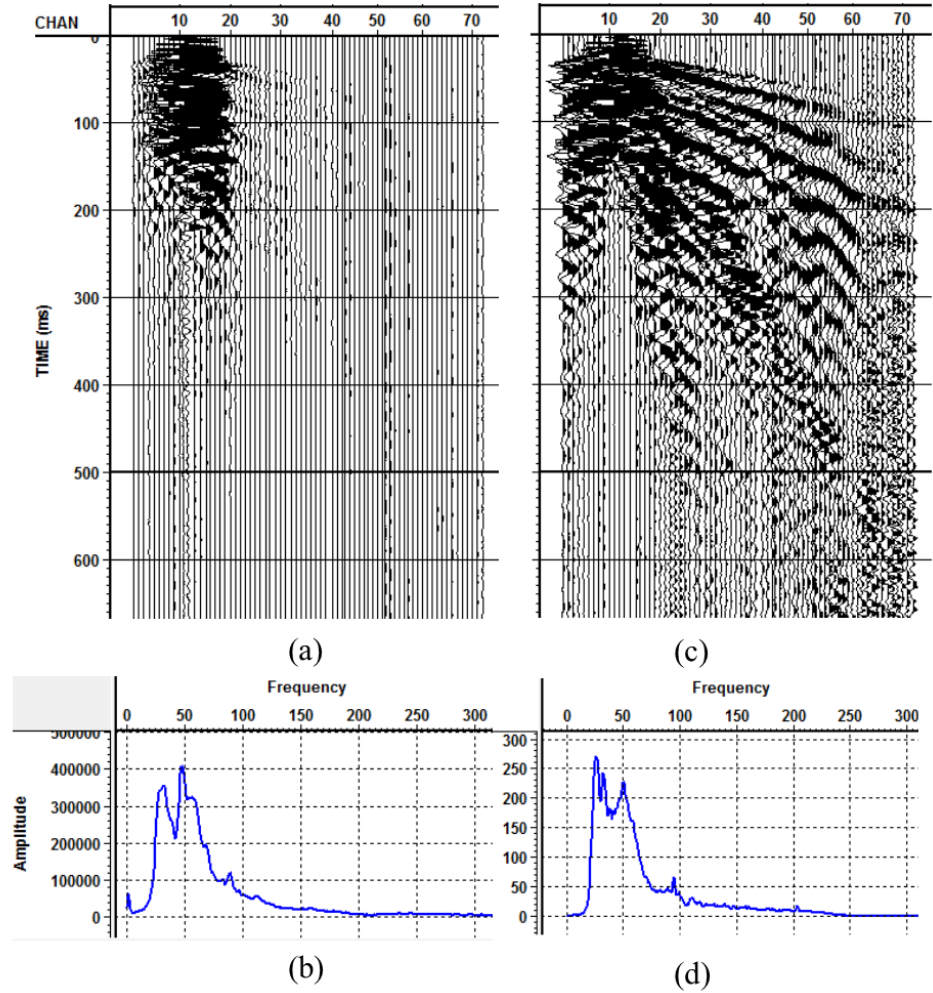
(a)

(b)

(c)

(d)

Figure B.14 shows example shot gather number 317 from Line MO-4, (a) raw shot record with its average amplitude spectrum (b) and (c) shot gather after geometry setting, static correction, amplitude scaling and recovery with exponential constant 0.25 to compensate for attenuation loss, FK filter and bandpass filter 10-20-200-250 Hz with its average amplitude spectrum in (d).
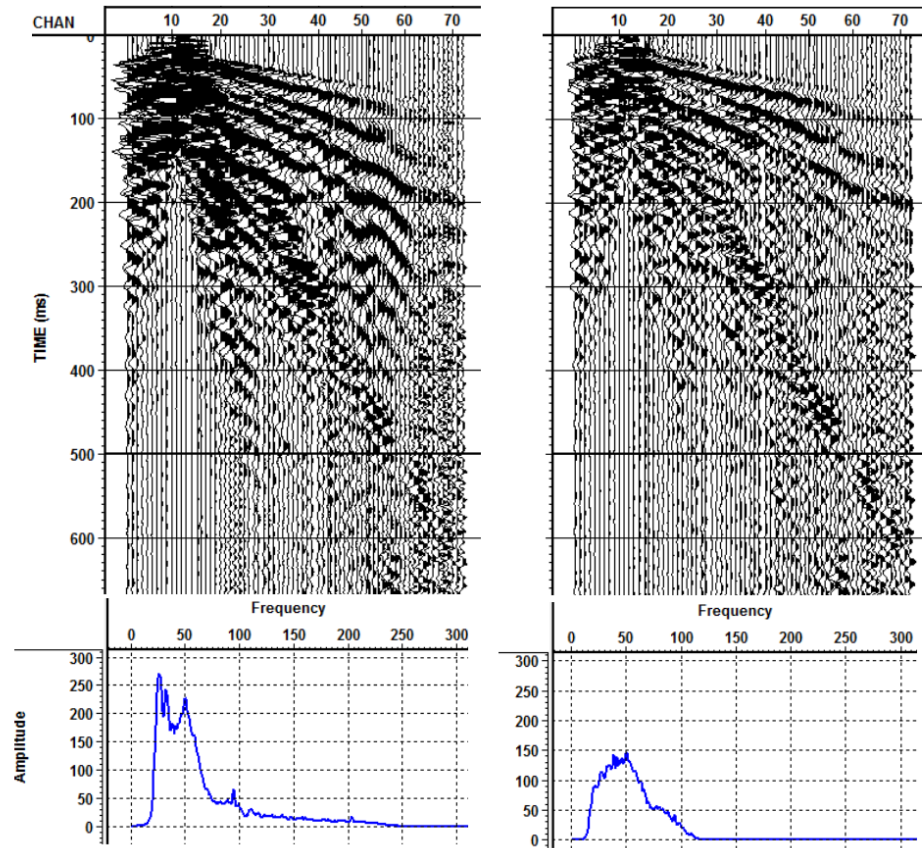
Shot 317

Figure B.15 displays the shot gather number 317 from survey Line MO-4 (left) after FK filter and (right) after predictive deconvolution with operator length 80 ms and predictive lag 20 ms and, (right) after frequency filter 10-20-90-120 follow by mean scaling and bottom mute.

APPENDIX C

Resistivity and MASW Methods

Methodology: Electrical Resistivity survey

The resistivity survey was acquired with ABEM Terrameter SAS4000 resistivity-meter (ABEM Instrument AB, 2012). The dipole-dipole configuration, that has comparatively high sensitivity and very good noise rejection circuitry, were used with electrode spacing 5 m. The RES2DINV inversion demo program (Loke, 1998) read the field apparent resistivity values and inverted that to create the calculated apparent resistivity carried out from 2D true resistivity model with least-squares method. The iteration of least-squares inverse routine was applied to properly match between a field apparent resistivity and calculated apparent resistivity. Figure C.1a presents the true electrical resistivity model resulted from the inversion process with the 10 iteration calculations and final 5% RMS error.

Methodology: Multichannel Analysis of Surface Waves

The MASW (MASW, 2017) focus on surface waves that have velocity dispersion property effected from subsurface layering contribution to velocity variation with frequency. Because surface wave have lower frequency contents then reflected wave, to capture more surface wave energy, the 4.5 Hz frequency respond geophones were employed. The surface shot gathers were recorded with 24 channels per shot, 2 m geophone spacing, 4 m shot spacing and the distance 8 m between shot location and the first geophone. The MASW data were analyzed by software called ParkSEIS (PS) (Park Seismic LLC, 2015). The field records were transformed into phase velocity spectrum for dispersion analysis to estimate the fundamental mode dispersion curves. The iteration of least-squares inverse routine was applied to properly match between picked dispersion curve and calculated dispersion curve which carry out from measurement and initial

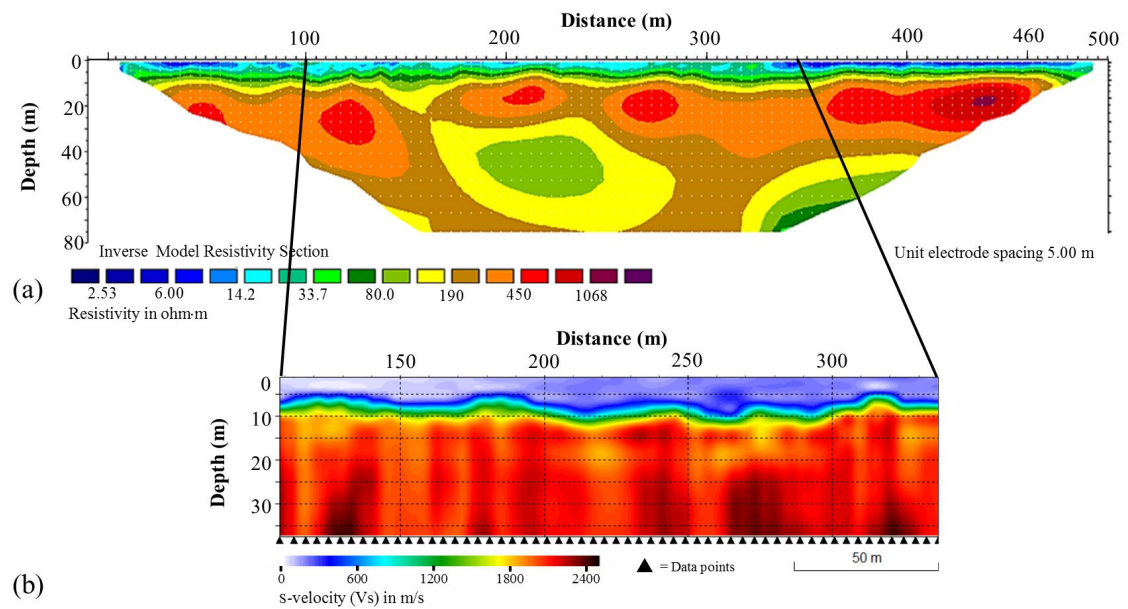model respectively. The solution from MASW method is the 2D S-wave velocity model displayed in Figure C.1b.

Figure C.1   shows (a) true electrical resistivity model and (b) S-wave velocity model from Line MO-2.

CURRICULUM VITAE

Author's Name   Miss Srivipa Lerkrattanawaree

Date/Year of Birth   15 March 1991

Place of Birth   Bangkok

Education   2013 Bachelor degree of Science, Geoscience, Mahidol
                       University, Kanchanaburi, Thailand.

Scholarship   2010 to Presents   the Science Achievement Scholarship of
                       Thailand (SAST)